

Article

Enhancement of Photoelectrochemical Cathodic Protection of Copper in Marine Condition by Cu-Doped TiO₂

Pailin Ngaotrakanwivat ^{1,2,*}, Piyapol Heawphet ¹ and Pramoch Rangsunvigit ^{3,4,*} 

¹ Department of Chemical Engineering, Burapha University, Chonburi 20131, Thailand; Piyapolheawphet@gmail.com

² Research Unit of Developing Technology and Innovation of Alternative Energy for Industries, Burapha University, Chonburi 20131, Thailand

³ The Petroleum and Petrochemical College, Chulalongkorn University, Bangkok 10330, Thailand

⁴ Center of Excellence on Petrochemical and Materials Technology, Bangkok 10330, Thailand

* Correspondence: pailin@eng.buu.ac.th (P.N.); Pramoch.r@chula.ac.th (P.R.); Tel.: +66-2218-4135 (P.R.)

Received: 11 December 2019; Accepted: 20 January 2020; Published: 22 January 2020



Abstract: Photochemical cathodic protection (PEC) efficiency was enhanced by doping TiO₂ with Cu (Cu/TiO₂) through impregnation and reduction under hydrogen. The Cu loading was varied from 0.1 to 1.0 mol% (0.1 Cu/TiO₂, 0.5 Cu/TiO₂, 1 Cu/TiO₂). Then, up to 50 wt% Cu/TiO₂ was mixed with TiO₂ to form nanocomposite films. The film photocurrent and photopotential were measured under 1 mW/cm² UV irradiation. The Cu/TiO₂ film with 10 wt% of 0.5 Cu/TiO₂ exhibited the highest photocurrent of 29.0 mA/g, which was three times higher than the TiO₂ film. The underlying reason for the high photocurrent was the lower photopotential of film than the corrosion potential of copper for PEC. This film was also applied on copper terminal lug for anti-corrosion measurement by Tafel polarization in 3.5 wt% NaCl solution. The results showed that the photopotential of terminal lug coated with the film was −0.252 V vs. Ag/AgCl, which was lower than the corrosion potential of copper (−0.222 V vs. Ag/AgCl). Furthermore, the film can protect the corrosion of copper in the dark with 86.7% lower corrosion current (*i*_{corr}) than that of bare copper.

Keywords: TiO₂; Cu; anti-corrosion; photoelectrochemical cathodic protection

1. Introduction

Copper has been playing a vital part in many aspects in this modern world, e.g., renewable energy, conductive materials, and construction materials, owing to its promising electronic, thermal, mechanical, and chemical properties. Global demand of copper was projected to be 36 million metric tons with \$261 billion market size in 2019 [1]. However, copper can be easily corroded, especially in the current rapid change in the environment [2].

Commonly known corrosion prevention methods include using electrical current and installing a sacrificial or non-sacrificial anode. The techniques inherit a few disadvantages, like cost of electricity and periodical maintenance. Photoelectrochemical cathodic protection (PEC) has emerged as a viable candidate for metal protection and has been considered as a green and non-polluting sacrificed anode. The principle of PEC is to provide photo-generated electrons to compensate the loss of electrons in a protected metal, which retains the potential to be lower than its corrosion potential. Specific semiconductors have been used as a non-sacrificial anode. They must generate photo-excited electrons under appropriate light. Their conduction band must be lower than the corrosion potential of protected metal. The photo-excited holes must oxidize a hole-trapping agent in like water to inhibit the e[−]-hole recombination. Last but not least, the semiconductors must be stable [3].

One of outstanding materials for PEC is titanium dioxide (TiO_2) owing to high chemical resistance and bandgap energy that is sufficiently wide to initiate an oxidation of water; however, TiO_2 can only be activated by the UV light, which is only 5% in the solar energy distribution [4]. A good example of using TiO_2 in the PEC is to prevent corrosion of 304-stainless steel in 300 ppb H_2O_2 aqueous solution. By coating the steel with TiO_2 film, the photopotential of the coated surface under 17 mW/cm^2 UV intensity was at 0.168 V vs. SHE, which was lower than that of bare 304-stainless steel (0.184 V vs. SHE). Moreover, the corrosion current was decreased to 79% of the corrosion current of bare 304-stainless steel [5].

Another advantage of using TiO_2 in the PEC is the harvesting ability of TiO_2 . The light harvesting efficiency of TiO_2 can be improved by reduction of the energy bandgap to extend the range of appropriate light and to suppress e^- -hole recombination to increase photo-excited electron production. TiO_2 particles doped with 5–15 mol% Cu were reported to have a higher photocurrent than pristine TiO_2 under a solar simulator. The 5 mol% Cu-doped TiO_2 particles exhibited the maximum photocurrent, 0.16 mA, under 100 mW/cm^2 solar radiation intensity. Thus, Cu-doped TiO_2 is a good candidate for photodiode and photodetector application [6]. Up to today, Cu-doped TiO_2 has not been used as a coating material for anti-corrosion by PEC.

The aim of this study was then to synthesize Cu-doped TiO_2 particles with superior photocurrent to pristine TiO_2 . The particles were then mixed with TiO_2 to form nanocomposite films. The nanocomposite films were assembled for photoelectrochemical cathodic anti-corrosion of copper terminal lug in the marine condition.

2. Results and Discussion

Figure 1 shows XRD of Cu/ TiO_2 with different Cu loadings. The diffraction peaks of pristine TiO_2 are in accordance with the standard structure of the anatase and rutile (JCPDS 21-1272 and JCPDS 21-1276, respectively). The diffraction patterns of TiO_2 doped with Cu in the range of 0.1–1 mol% are the same as the pristine TiO_2 . However, the higher the Cu content, the lower the diffraction peak intensity, implying the lower crystallinity of Cu/ TiO_2 . Moreover, the main diffraction peaks of both anatase and rutile are shifted towards lower angles, as shown in the insertion No. 1 and No. 2, respectively. The evidence emphasizes the successful substitution of Cu atoms into the TiO_2 lattice, accordingly [7,8].

First, the as-prepared Cu/ TiO_2 particles were fabricated as a film on ITO glass. Photocurrent and photopotential of Cu/ TiO_2 films were examined with 1 mW/cm^2 UV intensity, and the results are shown in Figure 2. It is evidence that the photocurrent of Cu/ TiO_2 films is higher than that of pristine TiO_2 film. This implies that the Cu/ TiO_2 films could effectively supply photo-excited electrons in order to protect metal from corrosion better than the pristine TiO_2 film. In addition, the photocurrent increases with the increase in the Cu doping. However, when the Cu content is greater than 0.5 mol%, the photocurrent decreases. This could be the result from the excess loading of $\text{Cu}(\text{NO}_3)_2$ in the TiO_2 particles that could not be totally reduced. It is worth noting that the presence of copper in the TiO_2 particles results in higher photocurrent, substantiating the interaction between copper and TiO_2 . However, the reduced $\text{Cu}(\text{NO}_3)_2$ particles do not have any photocurrent. This similar evidence was also previously reported [8].

Whether the Cu/ TiO_2 film is a potential anti-corrosion material lies in its photo potential that should be lower than the corrosion potential of copper metal ($E_{\text{corr}} = -0.222 \text{ V vs. Ag/AgCl}$). With this specific property, the photo-excited electrons could then be transferred to the metal in order to compensate the loss of electrons under corrosive environment. However, the results show that the photopotential of Cu/ TiO_2 films is higher than the corrosion potential of copper metal. In addition, the higher loading of Cu in the Cu/ TiO_2 film exhibits higher photopotential because of the coexistence of Cu from the reduction of $\text{Cu}(\text{NO}_3)_2$. An appropriate film with lower photopotential than corrosion potential and, at the same time, with higher photocurrent than the pristine TiO_2 particles is needed.

To achieve that, a material with lower potential such as TiO_2 is then incorporated to form nanocomposite film with different $\text{Cu}/\text{TiO}_2:\text{TiO}_2$ weight ratio.

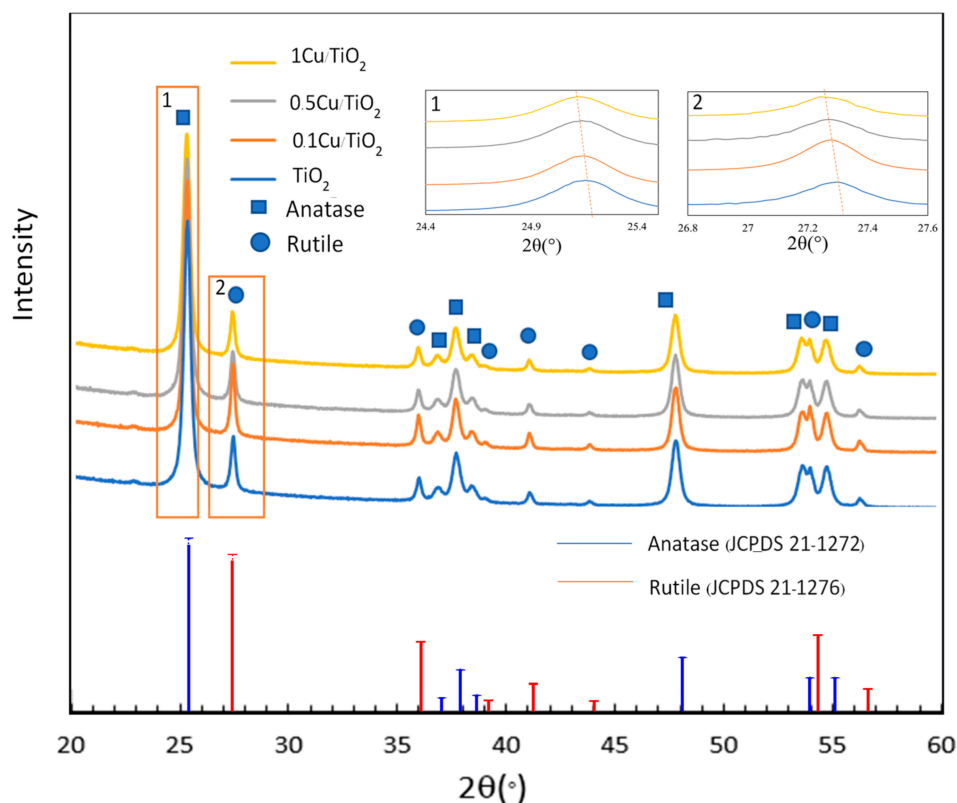


Figure 1. Patterns of Cu/TiO_2 particles at various Cu loadings.

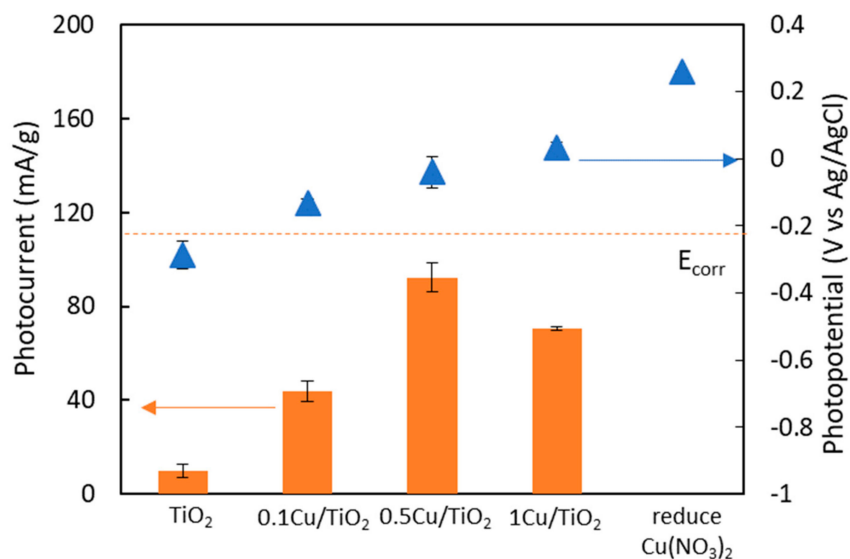


Figure 2. Photocurrent and photopotential of Cu/TiO_2 films under UV irradiation.

The morphologies of 0.5 Cu/TiO_2 10 and 1 Cu/TiO_2 50 composite films are illustrated in Figure 3. It can be seen that the existence of spherical nanoparticles with a diameter up to 30 nm in the porous composite films (Figure 3E,G,I,K) is similar to the morphology of TiO_2 film (Figure 3A). These nanoparticles should be the TiO_2 particles due to the major elements of particles are Ti and O in

the appropriate stoichiometric ratio of TiO_2 , as shown in Table 1. Moreover, the particle size of nanoparticles is in accordance with the particle size of Degussa P25 (~21 nm). Surprisingly, the larger spherical particles with the diameter up to 800 nm only exist in the composite films (area d in Figure 3E, area f in Figure 3G, area h in Figure 3I, and area j in Figure 3K), whereas the large spherical particles are not in the TiO_2 film (Figure 3A). It might be the agglomeration of Cu/TiO_2 particles containing in the film. The EDX measurement further substantiates the above hypothesis. The composition of element in the nanocomposite films is shown in Table 1.

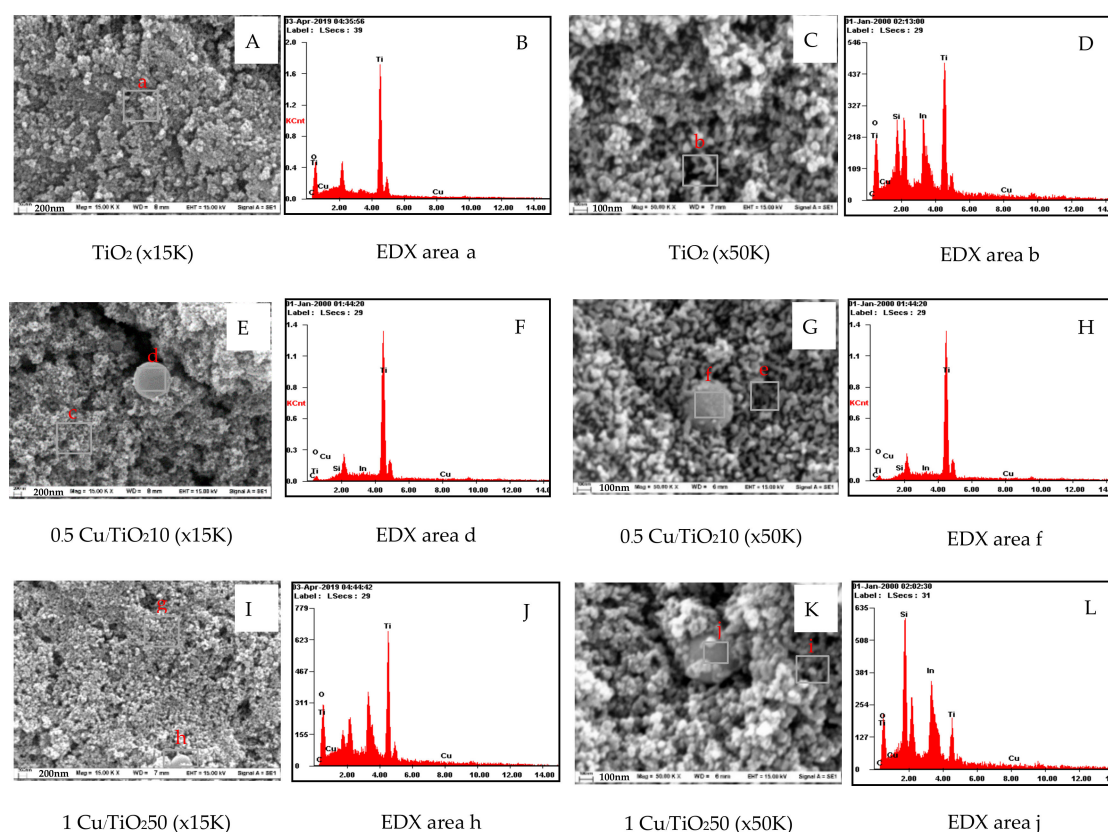


Figure 3. Scanning electron micrographs of $\text{Cu/TiO}_2\text{-TiO}_2$ composite films (A,E, and I (magnification: $\times 15\text{ K}$) and C,G, and K (magnification: $\times 50\text{ K}$) and EDX spectrum of the $\text{Cu/TiO}_2\text{-TiO}_2$ composite films (B,D,F,H,J,L).

Table 1. Average percentage of element in the nanocomposite films.

Element (%)	TiO ₂ Film	0.5 Cu/TiO ₂ 10 Film		1 Cu/TiO ₂ 50 Film	
	Area (a, b)	Area (c, e)	Area (d, f)	Area (g, i)	Area (h, j)
Ti	29.61	57.13	55.02	17.35	14.88
Cu	0.82	1.34	0.86	1.67	2.24
O	66.19	39.36	41.41	74.57	74.96
C	3.38	2.17	2.72	6.41	7.92
sum	100	100	100	100	100
Cu/Ti	0.03	0.02	0.02	0.10	0.15

It can be seen that the Cu/Ti molar ratio of the large spherical particles in the 1 $\text{Cu/TiO}_2\text{50}$ film (area h in Figure 3I and area j in Figure 3K) is 0.15, which is 1.5 times larger than that in the porous area (area g in Figure 3I and area i in Figure 3K). This indicates the possibility of the formation of Cu/TiO_2 particles. It should be noted that although the Cu/Ti molar ratio of the porous area (area g in Figure 3I and area i in Figure 3K) is larger than that of the TiO_2 film, the possibility of hidden Cu/TiO_2 under

the porous area might be the reason. Furthermore, the measured Cu/Ti molar ratio is greater than the prepared Cu/Ti mole ratio, which might be caused by sintering of Cu nanoparticles during the reduction in H₂ atmosphere at 400 °C [9]. However, the difference of the Cu/Ti mole ratio in the areas c and d in Figure 3E cannot be observed. This similar trend is observed in the areas e and f in Figure 3G. This might be the limitation of equipment for the detection of trace amount of Cu.

The band gap energy of nanocomposite films containing various doping amounts of Cu was obtained from the diffuse reflectance measurement. The Cu/TiO₂-TiO₂ films reflect the indirect band gap energy as shown in Figure 4. The band gap energy is determined from the dependencies of $(F(R)h\nu)^{1/2}$ against photon energy. However, the TiO₂ film exhibits the direct band gap energy as the insertion in Figure 4; thus, the intersection of the extrapolated linear portion of $(F(R)h\nu)^2$ vs. photon energy indicates the band gap energy of TiO₂ film.

The Cu dependence of energy band gap is plotted in Figure 5. The energy band gap of films containing Cu at 63, 313, 627, 1566, and 3135 µg/g of TiO₂ are 2.88, 2.83, 2.76, 2.72, and 2.69 eV, respectively. These results illustrate the gradual reduction of the band gap energy with the increase in the Cu content in TiO₂. The lowering of band gap energy is the result from the reduction of Fermi level. This evidence is in accordance with the previous work [7]. Therefore, the composite films with lower band gap energy should effectively generate electrons. It is worth noting that the films with the same amount of Cu (0.1 Cu/TiO₂50, 0.5 Cu/TiO₂10, 1 Cu/TiO₂5) exhibit almost the same band gap energy (2.85, 2.83, 2.80 eV), although the copper density in these three films is different.

The photocurrent of films having different band gap energy was further investigated, and the results are in Figure 6. Although it is generally accepted that the decrease in the band gap energy is proportional to the increase in the photocurrent [10], the increase in the Cu content increases the photocurrent up to 313 µg in 1 g of TiO₂ particles; however, further increase in the Cu hardly affects the photocurrent. This phenomenon is in good agreement with the results reported by Yildirim [6].

Particularly, three films containing the equivalent copper content at 313 µg/g of TiO₂ (0.1 Cu/TiO₂50, 0.5 Cu/TiO₂10, 1 Cu/TiO₂5) exhibit the identical energy band gap with significantly different photocurrent. This is attributed to the difference in the rate of electron generation and the rate of electron-hole recombination of those films. The film consisting of 50 wt% of 0.1 Cu/TiO₂ particles could generate a larger number of photoexcited electrons than that with 10 wt% of 0.5 Cu/TiO₂ particles and 5 wt% of 1 Cu/TiO₂ particles, respectively. However, the electron generation ability of 0.5 Cu/TiO₂ particles is greater than that of 1 Cu/TiO₂ particles and 0.1 Cu/TiO₂ particles as mentioned in Figure 2. Furthermore, the rate of electron-hole recombination of 0.1 Cu/TiO₂50 film (50 wt% of 0.1 Cu/TiO₂ particles and 50 wt% of TiO₂ particles) is higher than that of 0.5 Cu/TiO₂10 film (10 wt% of 0.5 Cu/TiO₂ particles and 90 wt% of TiO₂ particles) and 1 Cu/TiO₂5 film (5wt% of 1 Cu/TiO₂ particles and 95 wt% of TiO₂ particles), respectively, which were previously reported by Shi et al. [11] and Wang et al. [12].

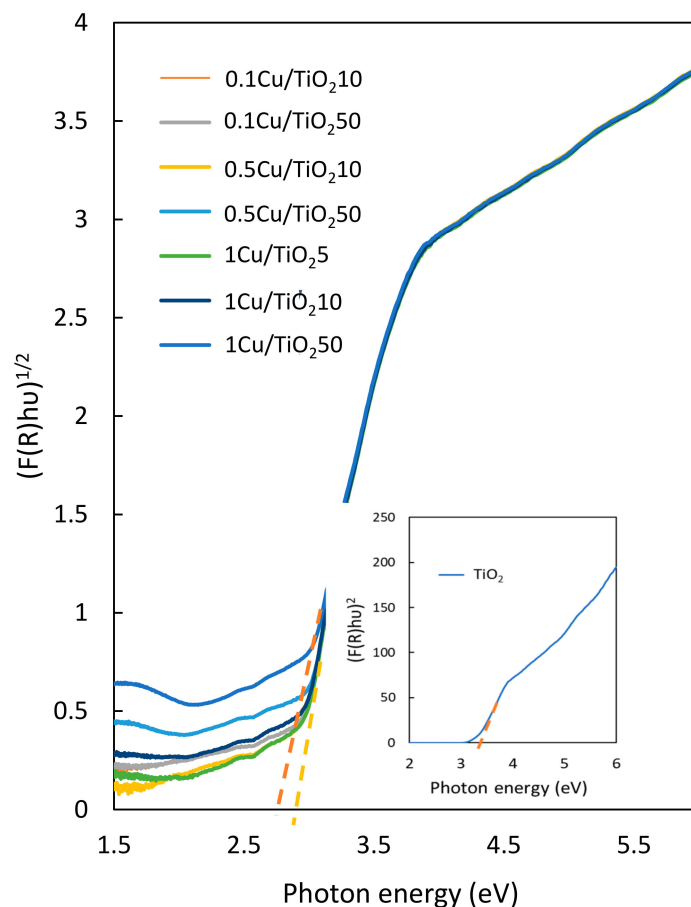


Figure 4. UV-Vis diffuse reflectance spectra of pristine TiO₂ and the nanocomposite films.

Photopotential of composite films with different Cu contents tends to increase with the increase in the Cu loading. However, the films consisting of Cu in the range of 0–313 $\mu\text{g/g}$ of TiO₂ show the sufficiently low photopotential for photoelectrochemical cathodic protection while the films containing Cu in the range of 313–3135 $\mu\text{g/g}$ of TiO₂ could not protect the copper from corrosion. It can be concluded that the optimum film condition is 0.5 Cu/TiO₂10 (313 μg Cu/g of TiO₂ particle), which has the highest photocurrent of 29 mA/g and photopotential of -0.26 V vs. Ag/AgCl. This particular film is then investigated for anti-corrosion efficiency.

Tafel polarization technique was employed to determine corrosion potential (E_{corr}) and corrosion current (i_{corr}) of copper terminal lug coated with composite films containing the equivalent Cu loading at 313 μg Cu/1 g of TiO₂ particle (0.1 Cu/TiO₂50, 0.5 Cu/TiO₂10, 1 Cu/TiO₂5) as in Figure 7. The terminal lug coated with 0.5 Cu/TiO₂10 and 1 Cu/TiO₂5 films have higher corrosion potential than those with 0.1 Cu/TiO₂50 and bare TiO₂, which is similar to the bare terminal lug as in Figure 7A. Generally, the higher potential than the corrosion potential can bring about the anti-corrosion enhancement [13]. It is worth mentioning that the potential shift to a higher value than the metal corrosion potential is proportional to the copper density in these films. Moreover, the corrosion currents (i_{corr}) of terminal lug coated with 0.5 Cu/TiO₂10 and 1 Cu/TiO₂5 films are 82.7% and 83.9% of corrosion current of bare terminal lug, respectively, as shown in Table 2. The decline of i_{corr} in the dark implies that the electron loss proceeds with difficulty.

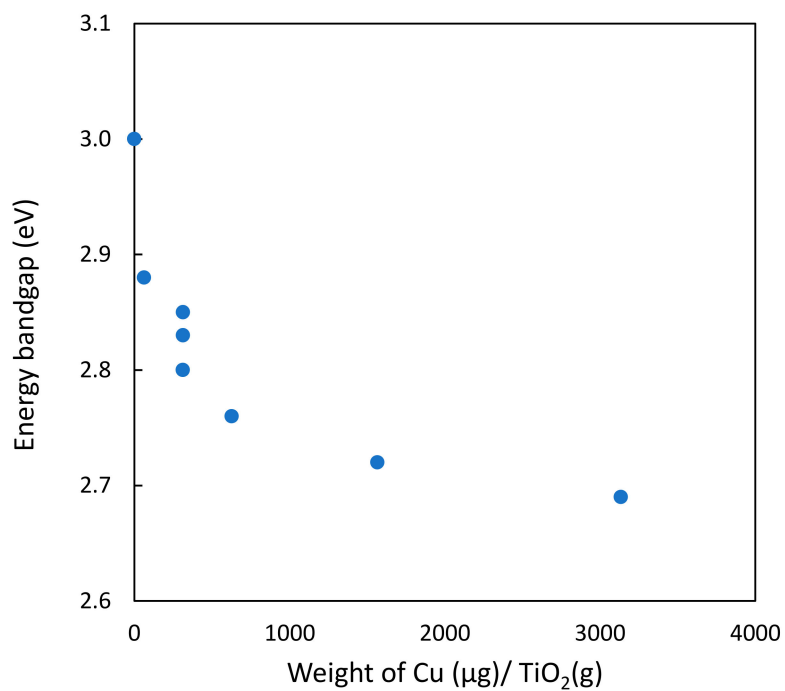


Figure 5. Cu loading dependence of energy band gap.

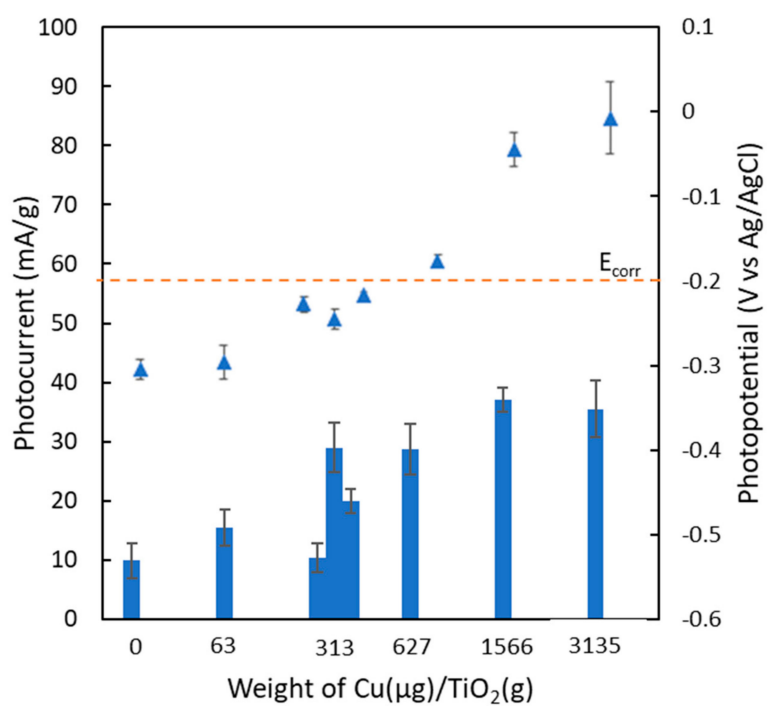


Figure 6. Dependence of Cu/Ti ratio on photocurrent and photopotential of composite films during UV irradiation at 1 mW/cm².

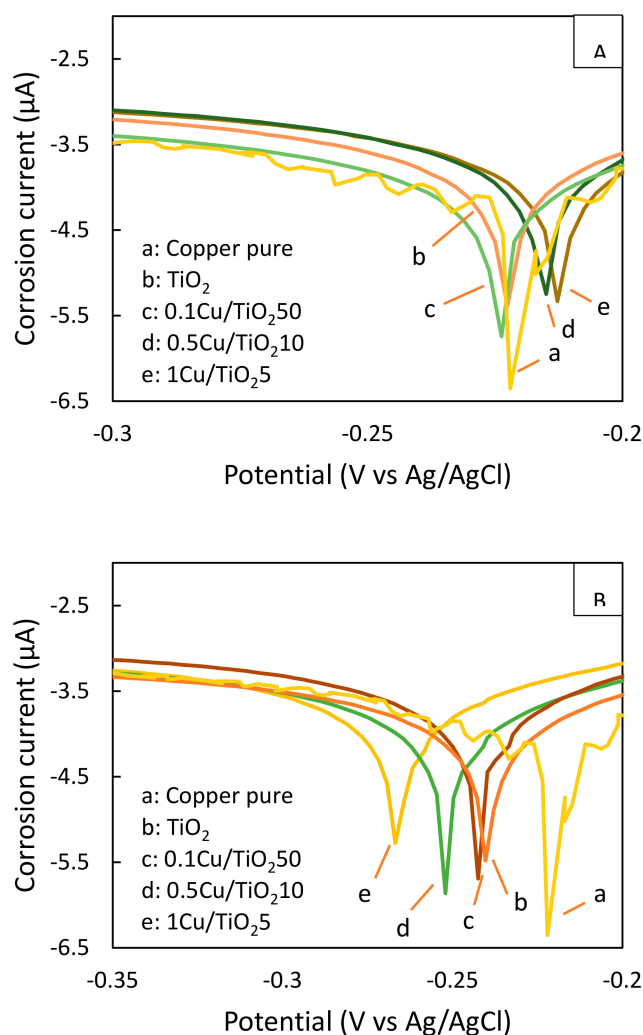


Figure 7. Polarization curves of copper terminal lug coated with nanocomposite films (A) in the dark (B) under UV irradiation at 1 mW/cm^2 .

Nevertheless, the terminal lugs coated with nanocomposite films and TiO₂ film have lower corrosion potential than the uncoated terminal lug under 1 mW/cm^2 UV irradiation, shown in Figure 7B. The higher the loading of TiO₂ particle in the film, the lower the negative corrosion potential is observed. However, the i_{corr} of coated terminal lug is not proportional to the decline in the photopotential. It is in accordance with the results of photocurrent of each film as discussed in Figure 6. The suitable film for photoelectrochemical cathodic anti-corrosion of copper terminal lug could be achieved with the 0.5 Cu/TiO₂10 film due to the E_{corr} of 0.5 Cu/TiO₂10 film is significantly shifted to -0.252 V , which is lower than the corrosion potential of bare terminal lug, with the highest i_{corr} at 89.6% of i_{orr} of bare terminal lug. The higher the i_{corr} under UV irradiation, the higher the number of photoexcited electrons can be generated, suggesting that a large number of generated electrons could compensate the electron loss to the environment.

It can be summarized that the increase in the density of Cu in the TiO₂ particles with the appropriate amount of TiO₂ particles ($>90 \text{ wt}\%$) plays an important role to raise the photocurrent up. These evidences emphasize that the coated terminal lugs could be protected from corrosion by the photoelectrochemical cathodic protection [14,15]. Therefore, the optimum nanocomposite film composition for anti-corrosion is 10 wt% of 0.5 Cu/TiO₂ with 90 wt% of TiO₂ particles. This film has the corrosion potential at -0.215 V and -0.252 V in the dark and under UV irradiation, respectively.

Unver UV irradiation, these films have higher corrosion current, 89.6%, than that of the bare copper terminal lug, while they have lower corrosion current, 82.7% in the dark.

Table 2. E_{corr} and i_{corr} of terminal lug coated with nanocomposite film.

	Cu/TiO ₂ in TiO ₂	E_{corr} (V)	ΔE_{corr} (mV)	i_{corr} (μA)	$i_{\text{corr}}/i_{\text{corr,copper}}$ (%)
	Copper pure	-0.222	0	6.35	100
Dark	TiO ₂	-0.224	2	5.74	90.4
	0.1 Cu/TiO ₂ 50	-0.222	0	5.38	84.7
	0.5 Cu/TiO ₂ 10	-0.215	7	5.25	82.7
	1 Cu/TiO ₂ 5	-0.213	9	5.33	83.9
Illuminated with UV light	TiO ₂	-0.240	-18	5.47	86.1
	0.1 Cu/TiO ₂ 50	-0.242	-20	5.69	89.6
	0.5 Cu/TiO ₂ 10	-0.252	-30	5.69	89.6
	1 Cu/TiO ₂ 5	-0.267	-45	5.28	83.2

3. Materials and Methods

Cu doped TiO₂ particles were prepared by wet impregnation. 6 mg of copper nitrate (Cu(NO₃)₂) precursor (DAEJUNG; purity 99%) were dissolved into 10 mL of ethanol (DAEJUNG; purity 99.5%) and the resulting solution was used for impregnation with 2 g of commercial TiO₂ particles (Degussa AEROXIDE P25). As-prepared powder was dried in the air at 80 °C for 5 h and reduced at 400 °C in the equimolar volumetric flow rate of H₂ (Linde; purity 99.99%) and N₂ (Linde; purity 99.99%) at 15 mL/min for 18 h. The obtained gray powder was designated as 0.1 Cu/TiO₂. The amount of copper nitrate in the impregnation was fivefold and 10-fold increased to obtain 0.5 Cu/TiO₂ and 1 Cu/TiO₂, respectively.

The as-prepared Cu/TiO₂ particles were further fabricated by coating the suspension on the indium-tin oxide (ITO) coated glass (surface area 3.1 cm²). The suspension consisting of 1 g of 0.1 Cu/TiO₂ particles, 30 mL of ethanol, and 0.25 mL of polyurethane (U202 Unithane Bager) were sonicated for 5 min. The gray slurry was sprayed onto the indium-tin oxide coated glass (ITO glass) as the substrate. The coated glass was then dried at 25 °C in the air for 5 h. In order to investigate the effect of copper amount doped in TiO₂ particles on photoelectrochemical cathodic protection, the equal amount of 0.5 Cu/TiO₂ and 1 Cu/TiO₂ was coated on the ITO glass, respectively.

The composite films with various weight ratios of Cu/TiO₂:TiO₂ affecting the photoelectrochemical cathodic protection were also investigated. The coating suspension of 0.1 Cu/TiO₂10 film was prepared by mixing of 0.1 g of 0.1 Cu/TiO₂ and 0.9 g of TiO₂ powder and dispersed in 30 mL of ethanol and 0.25 mL of polyurethane. In order to adjust the mole ratio, the composition of mixed powder was varied, and the resulting films are illustrated in Table 3.

The Cu/TiO₂-TiO₂ films were coated on the ITO coated glass (surface area 3.1 cm²) and copper terminal lug (surface area 5.2 cm²) by spray coating technique. The weight to area ratio was controlled on both substrates. The drying condition of all sample were prepared via the same procedure.

Table 3. Film composition at various weight ratios of Cu/TiO₂:TiO₂.

	Cu/TiO ₂ (g)	TiO ₂ (g)	Denoted as	Film Weight (mg/cm ²)
0.1 Cu/TiO ₂	0.1	0.9	0.1 Cu/TiO ₂ 10	0.51
	0.5	0.5	0.1 Cu/TiO ₂ 50	0.54
	1	0	0.1 Cu/TiO ₂	0.51
0.5 Cu/TiO ₂	0.1	0.9	0.5 Cu/TiO ₂ 10	0.57
	0.5	0.5	0.5 Cu/TiO ₂ 50	0.54
	1	0	0.5 Cu/TiO ₂	0.45
1 Cu/TiO ₂	0.05	0.95	1 Cu/TiO ₂ 5	0.54
	0.1	0.9	1 Cu/TiO ₂ 10	0.57
	0.5	0.5	1 Cu/TiO ₂ 50	0.55
	1	0	1 Cu/TiO ₂	0.48

The morphology and percentage of element in the Cu/TiO₂-TiO₂ films were characterized by scanning electron microscope (SEM) and energy dispersive x-ray (EDX) (Quanta400). The energy band gap was measured by UV-Vis spectroscopy (Shimadzu UV-1700). The phase of Cu/TiO₂ powder with various Cu contents was examined by a Rigaku X-ray diffractometer with Cu K α radiation ($\lambda = 0.15406$ nm) over the range $20^\circ < 2\theta < 60^\circ$.

The electrochemical techniques were implemented by assembling the coated glass or copper terminal lug in the three-electrode electrochemical cell: Coated glass or copper terminal lug as a working electrode, Ag/AgCl as a reference electrode, and platinum as a counter electrode filled with 3.5 wt% of NaCl (aq) as electrolyte. The film photocurrent was measured by a digital potentiostat (Autolab PGSTAT 302N) with chronoamperometry mode (bias potential as rest potential of film). The UV light source was a Hg-Xe lamp equipped with a 365 nm band-pass filter. The light intensity was about 1 mW/cm² at the sample surface. This particular light intensity was chosen to reflect the total solar ultraviolet radiation (TUV) in Thailand, which is in the range of 0–34 W/m² [16]. With this specific light intensity, the photoelectrochemical cathodic anti-corrosion could be effective for the whole day. Moreover, the film photopotential was measured by chronopotentiometry mode (bias current as zero A). Finally, Tafel polarization technique was employed to determine the cathodic protection both in the dark and UV irradiation.

4. Conclusions

This research successfully synthesized Cu-doped TiO₂ particle (Cu/TiO₂) at the optimum Cu doping condition 0.5 mol% in TiO₂ particles (0.5 Cu/TiO₂). The particles exhibited the photocurrent of 92.35 mA/g, which was nine times higher than conventional TiO₂. The nanocomposite film containing 0.5 Cu/TiO₂:TiO₂ at 10:90 was suitable for anti-corrosion of copper terminal lug in 3.5 wt% NaCl (aq) due to E_{corr} of copper terminal lug coated with that film being at −0.215 V vs. Ag/AgCl, which was higher than the bare terminal lug, and i_{corr} being at 82.7% of i_{corr} of bare terminal lug. Moreover, the photoelectrochemical cathodic protection was obtained with lower E_{corr} of copper terminal lug coated with the film (−0.252 V vs. Ag/AgCl) under UV irradiation with i_{corr} at 89.6% of i_{corr} of bare terminal lug. Therefore, the anti-corrosion of copper terminal lug could be achieved both in the dark and under UV irradiation.

Author Contributions: Conceptualization, P.N.; methodology, P.N.; validation, P.H. and P.R.; formal analysis, P.N. and P.R.; investigation, P.N., P.H. and P.R.; resources, P.N. and P.R.; data curation, P.H.; writing—original draft preparation, P.N. and P.H.; writing—review and editing, P.N. and P.R.; supervision, P.N.; project administration, P.N. and P.R.; funding acquisition, P.N. and P.R. All authors have read and agreed to the published version of the manuscript.

Funding: The financial supports from Faculty of Engineering, Burapha University (WJP 13/2556); Research Unit of Developing Technology and Innovation of Alternative Energy for Industries; Grant for International Research Integration: Chula Research Scholar, Ratchadaphiseksomphot Endowment Fund, Chulalongkorn University, Thailand; Center of Excellence on Petrochemical and Materials Technology (PETROMAT), Thailand; and The Petroleum and Petrochemical College, Chulalongkorn University, Thailand are gratefully acknowledged.

Acknowledgments: The authors would like to thank C&FC2019 organizing committee for the invitation to submit this work for consideration to be published in Catalysts.

Conflicts of Interest: The authors declare no conflict of interest. The funders had no role in the design of the study; in the collection, analyses, or interpretation of data; in the writing of the manuscript, or in the decision to publish the results.

References

1. Freedoniagroup. World Copper. Available online: <https://www.freedoniagroup.com/industry-study/world-copper-3274.html> (accessed on 3 October 2019).
2. Wan, Y. Corrosion behaviors of copper exposed to an urban atmosphere. *Int. J. Electrochem. Sci.* **2018**, *13*, 6779–6790. [CrossRef]
3. Bu, Y.; Ao, J.P. A review on photoelectrochemical cathodic protection semiconductor thin films for metals. *Green Energy Environ.* **2017**, *2*, 331–362. [CrossRef]
4. Rezaei, S.D.; Shannigrahi, S.; Ramakrishna, S. A review of conventional, advanced, and smart glazing technologies and materials for improving indoor environment. *Sol. Energy Mater. Sol. Cells* **2017**, *159*, 26–51. [CrossRef]
5. Wang, M.Y.; Li, T.H.; Yeh, T.K. Corrosion behavior of TiO₂-treated type 304 stainless steels in high temperature water containing with hydrogen peroxide. *J. Nucl. Sci. Technol.* **2015**, *53*, 666–672. [CrossRef]
6. Yıldırım, M. Characterization of the framework of Cu doped TiO₂ layers: An insight into optical, electrical and photodiode parameters. *J. Alloys Compd.* **2018**, *773*, 890–904. [CrossRef]
7. Dahlan, D.; Saad, S.K.M.; Berli, A.U.; Bajili, A.; Umar, A.A. Synthesis of two-dimensional nanowall of Cu-Doped TiO₂ and its application as photoanode in DSSCs. *Phys. E* **2017**, *91*, 185–189. [CrossRef]
8. Edelmannová, M.; Lin, K.Y.; Wu, J.C.S.; Troppová, I.; Čapek, L.; Kočí, K. Photocatalytic hydrogenation and reduction of CO₂ over CuO/TiO₂ photocatalysts. *Appl. Surf. Sci.* **2018**, *454*, 313–318. [CrossRef]
9. Ma, Z.; Liu, Y.; Shi, Q.; Zhao, Q.; Gao, Z. The mechanism of accelerated phase formation of MgB₂ by Cu-doping during low-temperature sintering. *Mater. Res. Bull.* **2009**, *44*, 531–537. [CrossRef]
10. Gao, L.; Du, J.; Ma, T. Cysteine-assisted synthesis of CuS-TiO₂ composites with enhanced photocatalytic activity. *Ceram. Int.* **2017**, *43*, 9559–9563. [CrossRef]
11. Shi, Q.; Ping, G.; Wang, X.; Xu, H.; Li, J.; Cui, J.; Abroshan, H.; Dinga, H.; Li, G. CuO/TiO₂ heterojunction composites: An efficient photocatalyst for selective oxidation of methanol to methyl formate. *J. Mater. Chem. A* **2019**, *7*, 2253–2260. [CrossRef]
12. Wang, D.; Pan, X.; Wang, G.; Yi, Z. Improved propane photooxidation activities upon nano Cu₂O/TiO₂ heterojunction semiconductors at room temperature. *RSC Adv.* **2015**, *5*, 22038–22043. [CrossRef]
13. Ammar, U.A.; Shahid, M.; Ahmed, M.; Khan, M.; Khalid, A.; Khan, Z. Electrochemical study of polymer and ceramic-based nanocomposite coatings for corrosion protection of cast iron pipeline. *Materials* **2018**, *11*, 332. [CrossRef] [PubMed]
14. Yu, S.Q.; Ling, Y.H.; Wang, R.G.; Zhang, J.; Qin, F.; Zhang, Z.J. Constructing superhydrophobic WO₃@TiO₂ nanoflake surface beyond amorphous alloy against electrochemical corrosion on iron steel. *Appl. Surf. Sci.* **2018**, *436*, 527–535. [CrossRef]
15. Dong, R.; Zhang, Q.; Gao, W.; Pei, A.; Ren, B. Highly efficient light-driven TiO₂-Au Janus micromotors. *ACS Nano* **2015**, *10*, 839–844. [CrossRef] [PubMed]
16. Buntoung, S.; Choosri, P.; Dechley, A.; Wattan, R.; Janjai, S. An investigation of total solar ultraviolet radiation at Nakhon Pathom, Thailand. *Procedia Eng.* **2012**, *32*, 427–432. [CrossRef]

